Research Repository UCD

Title	Synergistic effects of Bi/S codoping on visible light-activated anatase TiO2 photocatalysts from first principles
Author(s)	Long, Run; English, Niall J.
Publication Date	2009-04-20
Publication information	Journal of Physical Chemistry C, 113 (19): 8373-8377
Publisher	ACS Publications
Link to publisher's version	http://dx.doi.org/10.1021/jp900589k
This item's record/more information	http://hdl.handle.net/10197/2713
DOI	http://dx.doi.org/10.1021/jp900589k

Synergistic Effects of Bi/S Co-doping on Visible Light-Activated Anatase TiO$_2$ Photocatalysts from First-Principles

Run Long, Niall J. English[*]

The SEC Strategic Research Cluster and the Centre for Synthesis and Chemical

Biology, Conway Institute of Biomolecular and Biomedical Research, School of

Chemical and Bioprocess Engineering, University College Dublin, Belfield, Dublin 4,

Ireland.

Abstract: The electronic properties and photocatalytic activity of S and/or Bi-doped anatase TiO$_2$ are investigated by first-principles density functional theory calculations. For S-doped TiO$_2$, S 3p states locate above the top of the valence band and mix with O 2p states, leading to band gap narrowing. For Bi-doped anatase, the energy levels of the impurity Bi 6s states lie below the bottom of the conduction band while the Fermi level E_F lies above the gap states, indicating the gap states are fully occupied. The transition from Bi 6s to Ti 3d states is responsible for a red-shift of the visible light absorption edge. In Bi/S–doped TiO$_2$, both S 3p acceptor states and partially occupied Bi 6s donor states hybridized with S 3p appear simultaneously; this observation suggests that photocatalytic efficiency would be improved significantly due to greater separation of electron-hole pairs. These findings present a reasonable explanation of recent experimental results.

Keywords: Synergistic effect, electronic structure, codoping, TiO$_2$

---

[*] Corresponding author: Email: niall.english@ucd.ie, Tel. +353-1-716 1646, Fax: +353-1-716 1177

1. Introduction

TiO$_2$ has received intense attention due to its low cost, nontoxic, long-term stability and high oxidative power, which would render it one of the most promising materials in a wide range of technical fields, such as photocatalytic degradation of pollutants and photoelectrochemical conversion of solar energy.[1, 2] However, as a wide band gap semiconductor (e.g., 3.20 eV for anatase), TiO$_2$ can be only activated under UV-light irradiation, which accounts for only a small proportion (about 5%) of solar energy. Further, its photoexcited electron-hole pairs tend to recombine easily, which serves to limit further its utility as a photcatalyst. Therefore, in order to obtain highly effective photocatalysts, there has been a large focus on experimental attempts to 'engineer' the band gap of TiO$_2$ by various methods, such as doping with metal and nonmetals,[3-12] sensitizing by organic dyes,[13] and alloying.[14] Of these methods, doping seems one of the most effective. Though there have been many reports of TiO$_2$ doping by both metals and non-metal ions, reports of co-doped TiO$_2$ photocatalysts are substantially more rare. Recently, experimental work has shown that co-doping can enhance photocatalytic activity and the optical absorption region of TiO$_2$.[15, 16] **There are many theoretical studies focused on explaining the microelectronic mechanisms of either single-element doping, such as by C, N, S, Sn or codoping by nonmetal and metal elements.[17-22] In particular, the study of Gai et al. offers the possibility of modulating the band edges of TiO$_2$ to match visible light absorption through codoping by suitable nonmetal and metal elements.[22] To date, there are few studies concerned with Bi/S-doped TiO$_2$ used as visible light-activated**

photocatalysts, besides Wang et al.,[16] **which** reported that anatase co-doping with Bi and S can improve photocatalytic activity significantly and extend the absorption edge to 500-800 nm. They ascribed the highly active photocatalytic performance to arise from the existence of numerous oxygen vacancies, the acidic sites on the surface of TiO_2, and the high specific surface area. There are, however, no related theoretical studies investigating the effects of Bi/S co-doping. To understand the microscopic mechanisms of Bi/S co-doping on both crystal structure and the electronic structure, theoretical analysis by first-principles calculations is a valuable tool to study doping effects in detail. Therefore, it is desirable to investigate the origins of modifications to band structure and the enhancement of visible light activity of Bi/S-doped anatase.

The present work focuses on the electronic structure of (co-)doped anatase using density functional theory (DFT) calculations, and attempts to elucidate the origin of the experimentally observed synergistic effects of Bi/S doping leading to increased visible-light photocatalytic activity. Our theoretical analysis provides a possible explanation for the experimentally observed red-shift of the optical absorption edge and higher photocatalytic activity of Bi/S-doped TiO_2. We also discuss the thermodynamic properties of S-, Bi-, and Bi/S-doped anatase based on estimates of the formation energies.

2. Methodology and Systems

All of the spin-polarized density functional theory (DFT) calculations were performed using the Vienna *ab initio* Simulation Package (VASP).[23, 24] The

generalized gradient approximation (GGA) of the Perdew-burke-Ernzerhof (PBE) functional was adopted for the exchange-correlation potential.[25, 26] The electron wave function was expanded in plane waves up to a cutoff energy of 400 eV and a Monkhorst–Pack k-point mesh of $4 \times 4 \times 4$ was used for geometry optimization and electronic property calculations,[27] using the block Davidson scheme for geometry optimization. Both atomic positions and cell parameters were optimized until the residual forces were below 0.01 eV/Å.[28, 29] The optimized lattice parameters for pure anatase were $a = 3.800$ Å and $c = 9.483$ Å, in good agreement with experimental and other theoretical results,[30, 31] indicating that our simulation methodology was reasonable.

Doping systems were constructed from $2 \times 2 \times 1$ 48-atom anatase supercells. The S atom was substituted for an O atom and the Bi atom for a Ti atom. Bi/S-doped anatase was modeled by a single substitution of S for one O atom, and of one adjacent (nearest-neighbor) Ti atom replaced by substitution of a Bi atom per supercell. The free energy of this optimized configuration was evaluated to be some 0.3.eV lower than the next lowest free-energy optimized configuration, in which the Bi and S dopant atoms were as far apart as possible (one dopant in the center of the supercell with the other in a corner); a variety of different co-doping placement strategies were attempted. The atomic concentration of impurity was 2.08 %, which was comparable to that used in the experiment.[16] **To verify the effects of different doping levels of S and Bi on the electronic structure, further calculations were carried out for doped TiO$_2$ systems using a 96-atom supercell. The electronic structures of S-,**

Bi-, and Bi/S-doped TiO₂ at this doping concentration (half of that in the 48-atom case) showed nearly the same behavior as those found for the 48-atom supercell calculations. This suggests that our results are valid for the 48-atom supercell, in which interactions between dopants are negligible. The recent study of Gai et al also confirmed that the 48-atom supercell is sufficient to describe systems involving codoping between nonmetal and metal elements.[22] The supercell model is shown in Fig. 1.

3. Results and Discussion

3.1 Formation energy

To determine the relative stability of the doped systems, we calculated the formation energy. This can be thought of as quantifying the relative difficulty for doping by different ions in anatase, and is a widely used approach. The formation energies of substitutional S, Bi, and Bi/S dopants were calculated by

$$E_{form} = E(doped) - E(pure) - \mu_S - \mu_{Bi} + \mu_O + \mu_{Ti} \tag{1}$$

where $E(doped)$ is the total energy of the supercell containing the S, Bi, or Bi/S impurities, and $E(pure)$ is the total energy of the host pure TiO₂ supercell. μ_S and μ_{Bi} are the chemical potentials of impurity S and Bi, respectively. μ_O (μ_{Ti}) is the chemical potential for O (Ti). It should be noted that the formation energy is not fixed but depends on the growth conditions, which can be varied from Ti-rich to O-rich. For TiO₂, the chemical potentials of O and Ti satisfy the relationship $\mu_{Ti} + 2\mu_O = \mu(TiO_2)$. Under O-rich growth conditions, the chemical potential μ_O is determined by the

energy of an O$_2$ molecule ($\mu_O = \mu(O_2)/2$) and μ_{Ti} is determined by the formula above. Under Ti-rich conditions, μ_{Ti} amounts to the energy of one Ti atom in bulk Ti ($\mu_{Ti} = \mu_{Ti}^{metal}$) and then μ_O is calculated on the basis of the previous formula. For S and Bi impurities, the chemical potentials μ_S are determined by $\mu_S = \mu(SO_2) - 2\mu_O$. μ_{Bi} is found based on consideration of Bi$_2$O$_3$ (space group: P211/C1), using the relationship $2\mu_{Bi} = \mu(Bi_2O_3) - 3\mu_O$. The calculated formation energies are summarized in Table 1. Study of these results suggests that: 1) S prefers to occupy O sites under Ti-rich growth condition; 2) the incorporation of S promotes that of Bi under Ti-rich conditions. Therefore, the synthesis of Bi/S-doped TiO$_2$ is more favorable in comparison to single-Bi doping under the Ti-rich growth conditions in the experiment [16], although it still possesses a large formation energy. **It should be noted that the large ionic radii of S^{2-} (1.84 Å) and Bi^{3+} (1.03 Å) would result in high formation energies.[32] Introduction of a large S (Bi) atom into the interstitial site of the lattice induces large strain in the lattice about the dopant, and movement of the adjacent atoms. Although atomic relaxation reduces the formation energy for interstitial dopant configurations, the formation energy still remains high with values of 8.48 eV for S and 17.10 eV for Bi under Ti-rich conditions; therefore, interstitial S (Bi) defects are not energetically stable under normal conditions. In particular, simultaneous location of both S and Bi at interstitial sites leads to au unfavorable formation energy of 25.41 eV. Wang et al. also claimed that Bi is at the Ti sites in the lattice in their experimental samples,[16] while some researchers have suggested that S atoms were doped as anions to**

replace the lattice O atoms in TiO$_2$.[10] We also have found that simultaneous location of Bi and S at the Ti sites result in large formation energies of 24.43 eV under O-rich growth conditions and a higher value of 29.43 eV under Ti-rich conditions, indicating that S acting as a cationic dopant can hinder incorporation of Bi into the lattice. Consequently, we only discuss electronic structures for Bi and S as cationic and anionic dopants, respectively.

3.2 Electronic Properties

In order to compare the modifications of band gap and the origin of the observed red-shift in the absorption light edge with doping by different ions, we calculated the density of states (DOS) and the projected density of states (PDOS). They are plotted in Fig. 2. The calculated band gap of pure anatase TiO$_2$ is 2.0 eV, as shown in Fig. 2a, which is similar with to other theoretical results,[9] but underestimates the experimental value of 3.20 eV, due to well-known limitations of DFT. The band gap was found to broaden to 2.02, 2.06, and 2.06 eV for S-, Bi-, and Bi/S-doped TiO$_2$, respectively. For S-doped anatase (cf. Fig. 2b), it is shown clearly that acceptor levels of the S 3p states are slightly localized above the valence band maximum (VBM) O 2p states, and mixed with them to a certain extent, while the conduction band minimum (CBM) exhibits nearly no movement, leading to reduction in the band gap by 0.55 eV. This may be responsible for the experimentally observed red-shift in visible light absorption. Mixing between S 3p and O 2p states is a positive factor for transfer of carriers, as Asahi et al. emphasized.[8] The Bader charge on S was found to be -1.10 e,[33,]

[34] a reasonable result with substitutional doping of an S atom for an O atom. When one O atom was replaced by one S atom, three S-Ti bonds were observed to form. Two were of 2.170 Å in length and one was longer (2.350 Å), but both lengths were substantially larger than that of optimized lengths for O-Ti bonds in pure anatase (1.938 and 1.988 Å); this was due to the larger ionic radius of an S atom than that of an O atom. From Figs. 2b and 2b', the small peak on the upper edge of the valence band should be a bonding peak. The one at -0.5 eV is another bonding peak. It should be noted that longer bond lengths lead to weaker bond strengths as well as higher energy states. The two 2.17 Å bonds are σ-type between S 3p and Ti 3d, with a greater strength and lower energy level, while the single 2.350 Å bond possesses relatively weaker π-bond characteristics, with a higher energy level. They are all components of the valence band in S-doped TiO_2.

For Bi-doped TiO_2, the Bader charge on Bi was calculated to be 3e,[33, 34] indicating that the oxidization state of Bi ion is Bi^{3+}. **Before investigating the microscopic mechanism of alterations in band gap, it is necessary to analyze spin-related properties, because replacement of a Ti atom by Bi (having an odd number of electrons) introduces paramagnetic centers. Therefore, we plotted the spin density on the (100) plane for Bi-doped TiO_2 in Figure 3 (a). In this case, the unpaired electron is almost distributed on the adjacent O atoms with p states whereas substitutional Bi itself possesses a relatively small spin density with its s state, indicating the formation of Bi-O species. Although the experimental study did not report this,[16] it is speculated that the introduction of substitutional Bi**

into the TiO$_2$ lattice should result in a paramagnetic species. The DOS and PDOS show that the Bi 6s impurity states lie below the CBM with the formation of mid-gap states (Figs. 2c and 2c'). However, the Fermi level E$_F$ is above the Bi 6s gap states, indicating that the impurity states are fully occupied. The electron transition from Bi 6s states to the CBM is reduced by about 0.50 eV with respect to pure anatase, in agreement with the results for the reduction of the extent of the band gap to lie between the top of the Bi^{3+} 6s band and the bottom of the Ti^{4+} 3d band.[35] Thus the absorption spectra extend to longer wavelengths so that lower energy photons can be absorbed for photo-excitation, as observed experimentally.[16] When one Bi atom substitutes for one Ti atom, six O-Bi bonds were observed to form. Two were of 2.217 Å in length, while four were shorter (2.117 Å). Similar to the analysis for S-doped TiO$_2$, it was found that they were Bi 6s-O 2p anti-bonding. This indicates that electrons in the valence band can be excited to impurity states in the band gap in S- and Bi-doped TiO$_2$, and excited subsequently to the conduction band by absorption of visible-light. It is also possible that the impurity states at the VBM or CBM could act to reduce recombination rates of photo-excited carriers. Therefore, the impurity states would serve to promote the enhancement of photocatalytic efficiency.

For Bi/S-doped TiO$_2$ (cf. Figs. 2d and 2d'), the concomitant appearance of impurity states above the VBM and below the CBM consists of S 3p and Bi 6s states, respectively. The Fermi level E$_F$ is pinned to the tail of the Bi 6s states hybridized with S 3p, implying that the gap states are partially occupied. The distance between the acceptor S 3p levels and the donor levels above the E$_F$ is 1.12 eV, which is largely

responsible for the band gap reduction. The calculated results indicate clearly that S-Ti-O and O-Bi-Ti bonding lead to the presence of additional impurity states which can contribute to enhanced visible light absorption after the addition of Bi into S-doped TiO_2. In this case, the Bader charge of Bi is also 3 e but the value for S increases to -1.69 e. This value is more negative by about 0.59 e vis-à-vis the single S-doped system, because of attraction of more electrons from Bi and the adjacent Ti atoms. **In this case, the unpaired electron was centralized mainly on adjacent O atoms, while the Bi and S atoms had a relatively small spin density (cf. Figure 3(b)). O atoms exhibit p state character while Bi shows s state character. Further, the spin density is much less around the S atom than those of the O atoms because 3p orbitals are relatively further from nuclei vis-à-vis 2p orbitals. In other words, the spin density is localized around O atoms while it somewhat delocalized around S atoms. Therefore, the S atom does not possess simple p orbital characteristics, suggesting that there is hybridization between S atom and Bi atom; this is confirmed by the subsequent DOS and PDOS calculated results (see below).** For respective O and Ti replacement by S and Bi in the TiO_2 lattice, two S-Ti bonds and a single Bi-S bond were formed. Both of the S-Ti bonds lengths were 2.214 Å in length, while the S-Bi bond length was 2.543 Å, so that the average bond length was 2.324 Å; this is larger than the average S-Ti bond length of 2.23 Å in (single) S-doped TiO_2, moving the S 3p states to higher energies. In addition, four of the six Bi-O bonds lengths were 2.140 and 2.157 Å, while one was 2.205 Å and the longest was 2.543 Å; the average Bi-O bond length of 2.224 Å in the co-doped case

was larger than that of the average Bi-O bond length in single Bi-doped TiO_2 (2.150 Å). Therefore, one would expect Bi 6s states to move to higher energies upon co-doping, which is confirmed by the calculated DOS and PDOS (cf. Figs 2 c, c', d, d'). **A large possible benefit of codoping is the reduction of carriers' recombination rates with respect to monodoping.[22] However, experiments have reported that monodoping can act either to introduce recombination centers or to reduce the carrier mobility.[36, 37] In the case of codoping of Bi with S, the S atom modifies the valence band edge (characteristic of p-type doping), whereas the Bi atom modifies the conduction band (n-type doping). Given that the acceptor (S-dopant) and donor (Bi-dopant) states are both relatively shallow, they would serve to act as capture traps for photoexcited holes or electrons; their impurity energy levels near the VBM and CBM could reduce further the recombination rate of photoexcited carriers.[21] The Bi/S codoped system exhibits both shallow acceptor and donor states, and a much smaller separations between the S 3p and Bi 6s states vis-à-vis pure TiO_2. Tang et al have indicated that hybridization of impurity energy levels is favorable towards enhancing the lifetimes of photoexcited carriers;[38, 39] the observation in this study of hybridization between shallow Bi 6s and S 3p states suggests that separation between photoexcited electron-hole pairs would be enhanced further vis-à-vis monodoping.** This suggests that Bi and S co-doping is highly beneficial for the separation of photo-excited electron-hole pairs, and would serve to enhance the photocatalytic activity of anatase under visible light.

To verify that the conclusions drawn from our calculations are not affected by underestimated band gaps in standard DFT GGA calculations, we have performed further GGA + U calculations for pure TiO$_2$ and Bi/S-doped TiO$_2$.[40] The DFT + U method introduces an intra-atomic electron-electron interaction as an on-site correction in order to describe systems with localized d and f electrons. A value of 6.3 was chosen for the U−J parameter, based on the study of Gai et al.,[22] and this produced a very good band gap result of 3.14 eV for pure TiO$_2$. The calculated DOS and PDOS using the GGA + U method are presented in Figure 4. Although the band gap for Bi/S-doped TiO$_2$ is slightly larger with respect to the GGA calculated results, both approaches showed similar electronic properties, indicating that the GGA band gap differences in systems with and without dopants are similar.

4. Conclusion

We have calculated the electronic properties of S-, Bi, and Bi/S-doped anatase TiO$_2$ by means of density function theory calculations. The results indicate that single S doping reduces the band gap, driven by the mixing of S 3p and O 2p states, while single Bi ion doping produces midgap states which we suggest may be responsible for the experimentally observed red-shift of the optical absorption edge. In particular, our calculations suggest that Bi and S co-doping can reduce the band gap and enhance photocatalytic activity under visible light; shallow acceptor S 3p states and shallow donor Bi 6s states hybridized with S 3p were produced within the band gap, which

serve to enhance the separation of electron-hole pairs excited by photon irradiation. This could lead to substantial enhancements in photocatalytic activity of TiO_2 under visible-light, in agreement with recent experimental findings.[16]

References

(1) Linsebiger, A. L.; Lu, G. Q.; Yates, J. T. *Chem. Rev.* **1995**, *95*, 725.

(2) Fujishima, A.; Honda, K. *Nature* **1972**, *28*, 37.

(3) Herrmann, J. M.; Disdier, J.; Pichat, P. *Chem. Phys. Lett.* **1984**, *108*, 618.

(4) Choi, W.; Termin, A.; Hoffmann, M. R. *J. Phys. Chem.* **1984**, *98*, 13669.

(5) Yamashita, Y.; Ichiashi, M.; Taeuchi, S.; Kishiguchi, M.; Anpo, J. *Synchrotron Radiat.* **1999**, *6*, 451.

(6) Wang, Y. Q.; Cheng, H. M.; Zhang, L. et al. *J. Mol. Catal. A* **2000**, *151*, 205.

(7) Long, R.; Dai, Y.; Huang, B. B. *Comput. Mater. Sci.* **2009**, *45*, 223.

(8) Asahi, R.; Morikawa, T.; Ohwaki, T.; Aoki, K.; Taga, Y. *Science* **2001**, *293*, 269.

(9) Umebayashi, T. Yamaki, Y.; Itoh, H.; Asai, K. *Appl. Phys. Lett.* **2002**, *81*, 454.

(10) Umebayashi, T.; Yamaki,Y.; Yamamoto, S.; Miyashita, A.; Tanaka, S.; Asai, K. *J. Appl. Phys.* **2003**, *93*, 5156.

(11) Chen, D.; Yang, D.; Wang, Q.; Z. Jiang, Y. *Ind. Eng. Chem. Res.* **2006**, *45*, 4110.

(12) Sakthivel, S.; Kisch, H. *Angew. Chem., Int. Ed.* **2003**, *42*, 4908.

(13) Duncan, W. R.; Prezhdo, O. V. *J. Am. Chem. Soc.* **2008**, *130*, 9756.

(14) Lin, J.; Yu, J. C.; Lo, D.; Lam. S. K. *J. Cata.* **1999**, *183*, 368.

(15) Luo, H. M.; Gao, L. *Chem. Mater.* **2004**, *16*, 846.

(16) Wang, Y.; Wang, Y.; Meng, Y. L.; Ding, H. M.; Shan, Y. K.; Zhao, X.; Tang, X. Z. *J. Phys . Chem. C* **2008**, *112*, 6620.

(17) Di Valentin, C.; Pacchioni, G.; Selloni, A. *Chem. Mater.* 2005, *17*, 6656.

(18) Di Valentin, C.; Pacchioni, G.; Selloni, A.; Livraghi, S.; Giamello, E. J. Phys. *Chem. B* 2005, *109*, 11414.

(19) Umezawa, N.; Janotti, A.; Rinke, P.; Chikyow, Y.; G. Van de Walle, C.; *Appl. Phys.Lett.* 2008, *92*, 041104.

(20) Long, R.; Dai, Y.; Huang, B. B. *J. Phys. Chem. C* 2009, *113*, 650.

(21) Zhao, Z. Y.; Liu, Q. *J. Catal. Lett.* 2008, *124*, 111.

(22) Gai, Y. Q.; Li, J. B.; Li, S. S.; Xia, J. B.; Wei, S. H. *Phys. Rev. Lett.* 2009, *102*, 036402.

(23) Kresse, G.; Hafner, J. *Phys. Rev. B* **1993**, *47*, 558.

(24) Kresse, G.; Furtherműller, J. *Phys. Rev. B* **1996**, *54*, 11169.

(25) Perdew, J. P.; Burk, K.; Ernzerhof, M. *Phys. Rev. Lett.* **1996**, *77*, 3865.

(26) Perdew, J. P.; Wang, Y. *Phys. Rev. B* **1992**, *45*, 13244.

(27) Monkhorst, H. J.; Pack, J. D. *Phys. Rev. B* **1976**, *13*, 5188.

(28) Davidson, E.R. *Methods in Computational Molecular Physics* edited by G.H.F.

(29) Wilson, S. Vol. 113 *NATO Advanced Study Institute, Series C* (Plenum, New York, 1983), p. 95.

(30) Burdett, J. K.; Hughbandks, T.; Miller, G. J.; Richardson, J. W.; Smith, J. V. *J. Am. Chem. Soc.* **1987**, *10*, 3639.

(31) Lazzeri, M.; Vittadini, A.; Selloni, A. *Phys. Rev. B* **2001**, *63*, 155409.

(32) ***CRC Handbook of Chemistry and Physics 87th Edition*, edited by David R. Lide (Taylor & Franics, London, 2006).**

(33) Davidson, E. R. *Methods in Computational Molecular Physics* edited by G.H.F. Diercksen

(34) Wilson, S. Vol. 113 *NATO Advanced Study Institute, Series C* (Plenum, New York, 1983), p. 95.

(35) Rengaraj, S.; Li, X. Z.; Tanner, P. A.; Pan, Z. F. Pang, G. K. H. *J. Mol. Catal. A: Chem.* **2006**, *247*, 36.

(36) Irie, H.; Watanabe, Y. Hashimoto, K. *Chem. Lett.* 2003, *32*, 772.

(37) Hermann, J. M.; Disdier, J. Pichat, P. *Chem. Phys. Lett.* 1984, *108*, 618.

(38) Tang, J.; Zou, Z.; Ye, J. *Catal. Lett.* 2004, 92, 53.

(39) Tang, J.; Ye, J. *Chem. Phys. Lett.* 2005, 410, 104.

(40) Dudarev, S. L.; Botton, G. A.; Savarsov, S. Y.; Humphreys, C. J.; Sutton, A. P. *Phys. Rev. B* 1998, *57*, 1505.

Table 1 Formation energies E_{form} for S-, Bi-, and Bi/S-doped anatase, in eV.

		Ti-rich	O-rich
E_{form}	*S-doped*	*-5.12*	*9.88*
E_{form}	*Bi-doped*	*11.26*	*8.76*
E_{form}	*Bi/S-doped*	*5.29*	*17.79*

Figure Captions

Figure 1. Supercell model for Bi/S-doped anatase TiO_2 and the location of the dopants. The ion doping sites are marked with S and Bi. The large light balls and the small dark balls represent the Ti and O atoms, respectively.

Figure 2. (A) The density of states (DOS) for each of the simulated systems. (B) The projected density of states (PDOS). The top of valence band of pure anatase is taken as the reference level. The dashed lines represent the Fermi level, E_F.

Figure 3 Spin density maps on the (100) plane for (a) Bi-doped TiO_2 and (b) Bi/S-doped TiO_2.

Figure 4 (A) for DOS and (B) for PDOS for pure and Bi/S-doped TiO_2 from GGA + U calculations. The top of the valence band of pure TiO_2 is taken as reference level. The dashed lines represent the Fermi level, E_F.
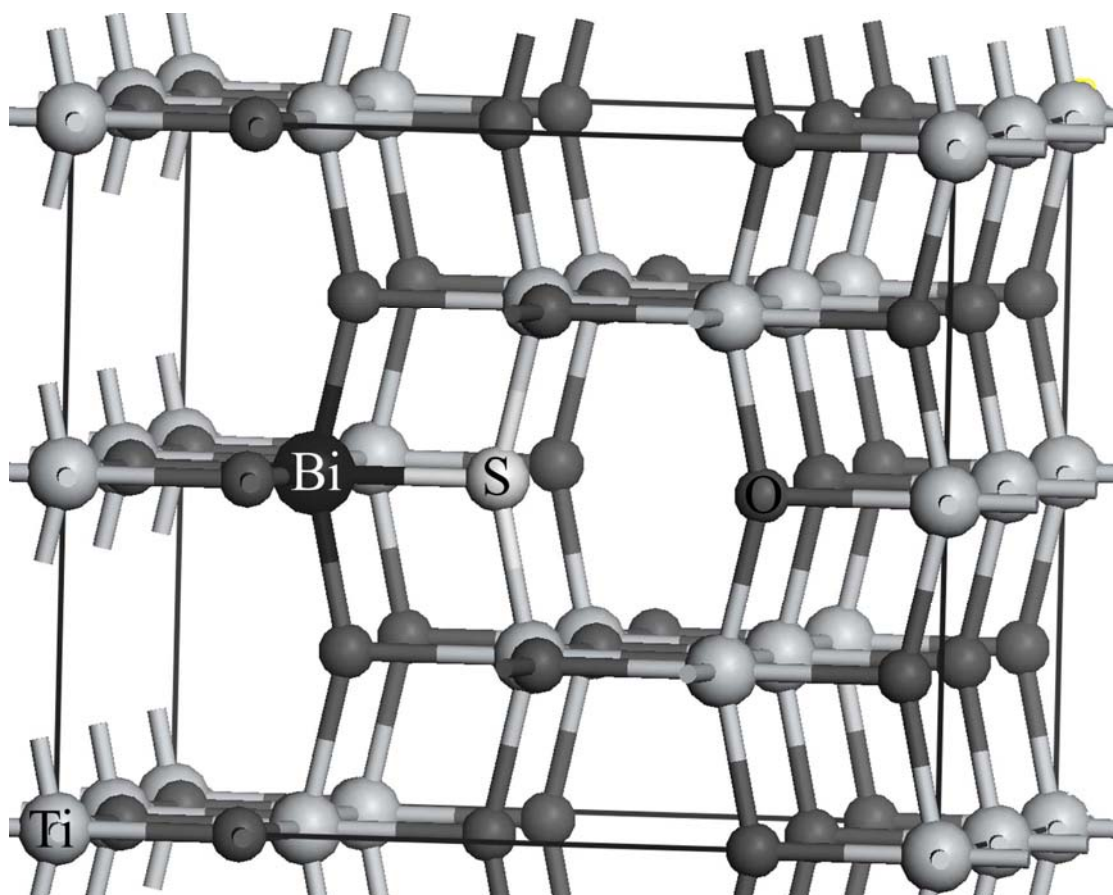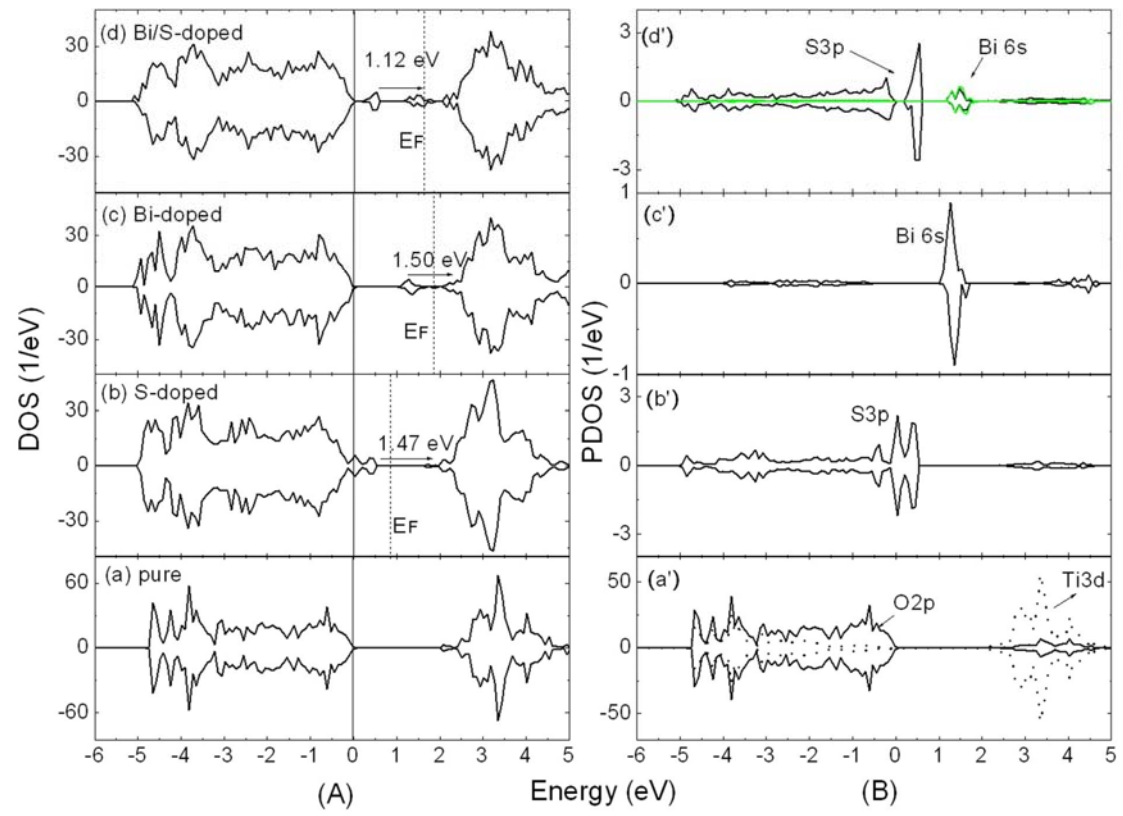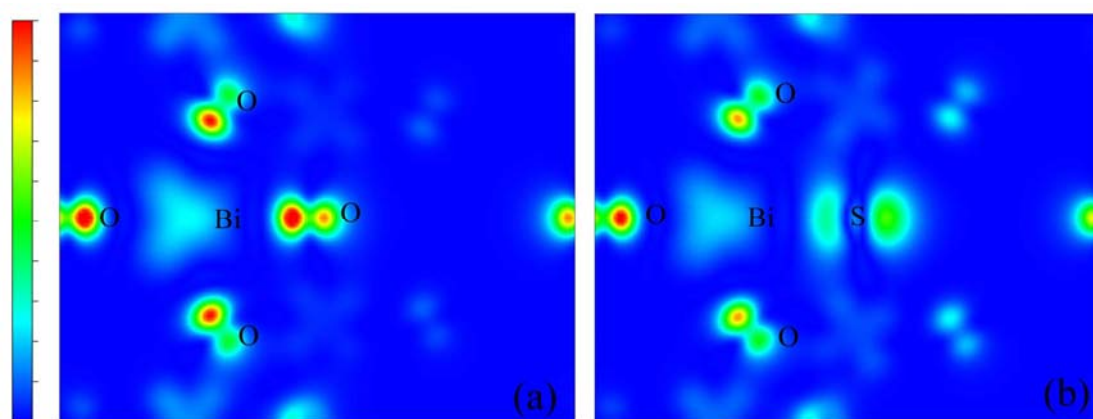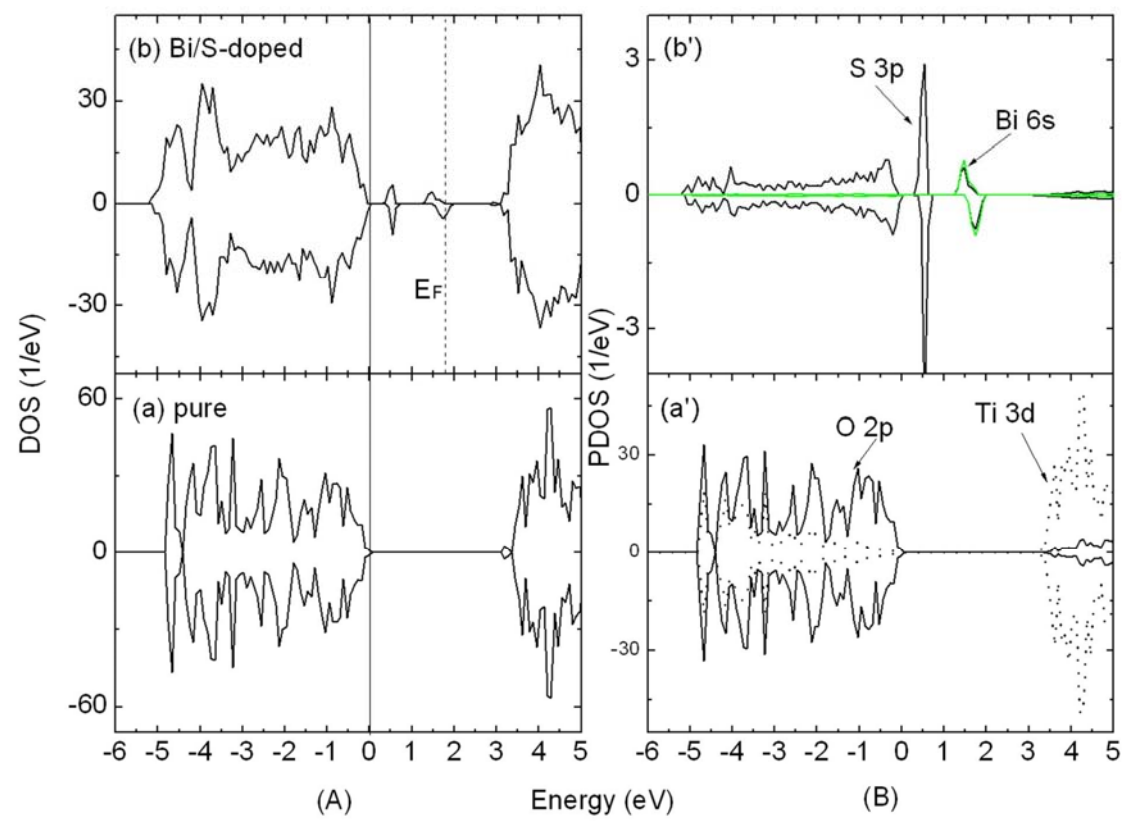
Figure 1

Figure 2

Figure 3

Figure 4